J. Fluid Mech. (1997), *vol.* 346, *pp.* 1–21. Printed in the United Kingdom

Transonic flow of dense gases around an airfoil with a parabolic nose

By ZVI RUSAK AND CHUN-WEI WANG

Department of Mechanical Engineering, Aeronautical Engineering and Mechanics, Rensselaer Polytechnic Institute, Troy, NY 12180-3590, USA

(Received 18 October 1996 and in revised form 9 May 1997)

Transonic potential flow of dense gases of retrograde type around the leading edge of a thin airfoil with a parabolic nose is studied. The analysis follows the approach of Rusak (1993) for a perfect gas. Asymptotic expansions of the velocity potential function are constructed in terms of the airfoil thickness ratio in an outer region around the airfoil and in an inner region near the nose. The outer expansion consists of the transonic small-disturbance theory for dense gases, where a leading-edge singularity appears. Analytical expressions are given for this singularity by constructing similarity solutions of the governing nonlinear equation. The inner expansion accounts for the flow around the nose, where a stagnation point exists. A boundary value problem is formulated in the inner region for the solution of an oncoming uniform sonic flow with zero values of the fundamental derivative of gasdynamics ($\Gamma = 0$) and the second nonlinearity parameter ($\Lambda = 0$) around a parabola at zero angle of attack. The numerical solution of the inner problem results in a symmetric flow around the nose. The outer and inner expansions are matched asymptotically resulting in a uniformly valid solution on the entire airfoil surface. In the leading terms, the flow around the nose is symmetric and the stagnation point is located at the leading edge for every transonic Mach number, and small values of Γ and Λ of the oncoming flow and any shape and small angle of attack of the airfoil. Furthermore, analysis of the inner region in the immediate neighbourhood of the stagnation point reveals that the flow is purely subsonic, approaching critical conditions in the limit of large (scaled) distances, which excludes the formation of shock discontinuities in the nose region.

1. Introduction

Recent years have shown an increased scientific and technological interest in the non-classical dynamics and real gas effects in compressible flows of dense gases. Dense gases are characterized as ordinary single-phase vapours of moderate molecular weight, operating at pressures and temperatures on the order of those corresponding to the thermodynamic critical point. At these conditions, the perfect gas law no longer holds and real gas effects should be carefully investigated. The research toward understanding the dynamics of dense gases is strongly motivated by their potential technological advantages, as working fluids, in Rankine cycle turbomachinery over the classical steam cycles (see the review paper on this subject by Devotta & Holland 1985). These benefits include increased efficiency and extended life cycle of turbines. Other applications may be found in the heavy-gas wind tunnel designed to get a better simulation for realistic high-Reynolds-number flows.

Specific interest has been developed in working fluids of retrograde type which

vaporize when compressed and condense when expanded. We particularly investigate those gases that are characterized by relatively large specific heats (c_v), known as the Bethe–Zel'dovich–Thompson (BZT) fluids (see Bethe 1942; Zel'dovich 1946; Zel'dovich & Raizer 1966; Thompson 1971; Thompson & Lambrakis 1973, Cramer & Tarkenton 1992). Recent research has shown that the physical behaviour of these kind of dense gases of retrograde type can be significantly different from the classical gasdynamics of perfect gases (see Cramer & Tarkenton 1992; Cramer & Fry 1993; Schnerr & Leidner 1993). Therefore, the ability to understand the complex phenomena that occur in compressible flows of dense gases and the parameters that govern them are scientifically interesting and would be essential for future utilization of these fluids in the design of advanced machinery and in aerospace applications.

In classical gasdynamics, the fluid is treated as a perfect gas. However, for dense gases operating in the single-phase vapour region near the phase boundary and at temperatures and pressures on the order of those of the thermodynamic critical point, real gas effects should be considered. Improved equations of state such as the van der Waals, Redlich–Kwong (1949) or Martin–Hou (1955) models should be used for a more accurate description of dense gas flows. One of the main parameters commonly used to describe the influence of real gas effects is the thermodynamic property

$$\Gamma = 1 + \frac{\rho}{a}\left.\frac{\partial a}{\partial \rho}\right|_s$$

where ρ, a, s are the density, isentropic speed of sound and specific entropy, respectively. A similar parameter was first introduced by Duhem (1909). Owing to its importance in a wide range of flow problems, Thompson (1971) referred to this parameter as the fundamental derivative of gasdynamics. This parameter may reflect the intrinsic gasdynamics nonlinearity. For a perfect gas model, $\Gamma = (\gamma + 1)/2$ is a constant and greater than 1 (here, $\gamma \geqslant 1$ is the ratio of specific heats). For dense gases Γ is no longer a constant, and may become less than 1 or even negative in a certain range of temperatures and pressures. Fluids, in the single-phase regime, of retrograde type (the BZT fluids) are characterized by $\Gamma < 0$ at densities on the order of one half to three quarters of the critical values and temperatures around the critical temperature (see figures 1 and 2 in Cramer & Tarkenton 1992). It is found that commonly used dense fluids, employed as heat transfer fluids or in Rankine cycle power systems, such as high molecular hydrocarbons and fluorocarbons can be identified as BZT fluids (a list of those fluids is given in Cramer 1989, 1991; Cramer & Tarkenton 1992 and Tarkenton & Cramer 1993).

Thompson (1971) was the first to examine near sonic one-dimensional flows of BZT gases in a duct. He showed that supersonic flow may be attained only by the way of a throat when $\Gamma > 0$, and by the way of an anti-throat (local maximum in the stream tube area) when $\Gamma < 0$. Thompson also suggested that a fluid with a constant negative Γ cannot be accelerated isentropically from stagnation to supersonic speeds and for such conditions a supersonic tunnel cannot be made. Compressible flows of the BZT fluids also show the non-classical result of the possible formation of expansion shocks, normally forbidden in the perfect gas theory. On the other hand, classical compression shocks are actually prohibited by the second law of thermodynamics when $\Gamma < 0$. These non-classical effects for a steady isentropic flow in a duct were explained by Cramer & Best (1991). A parameter $J = 1 - \Gamma - 1/M^2$ was introduced to describe the nonlinearity of the duct flow. It was found that in a perfect gas, or any other fluid with $\Gamma > 1$ as, specifically, $J < -1/M^2$, the Mach number decreases monotonically with the increase of density. Therefore, in such flows only compression shocks are

expected to occur. However, for any flow in a duct with $\Gamma < 1$, specifically for flows where $\Gamma < 0$, there exists a range of densities where J may become positive and the Mach number increases when the density increases. In such situations, the flow may accelerate to supersonic speeds in the regions of compression or the flow may expand from supersonic to subsonic speed and an expansion shock is, therefore, expected to occur.

The complex nature of transonic flows of BZT fluids is also found in the nozzle flow studies of Cramer & Fry (1993) and Kluwick (1993). Newly revealed phenomena included the existence of expansion shocks that stand upstream of the throat and flows which contain two or three shocks but no supersonic points. Both phenomena require the existence of sonic shock waves, i.e. shock waves for which the Mach number is identically 1 upstream or downstream of the shock, and are only possible when Γ changes its sign.

Transonic flows of BZT fluids around profiles have recently been studied by Cramer & Tarkenton (1992), Tarkenton & Cramer (1993). They presented an extended transonic small-disturbance theory for flows around thin airfoils of thickness ratio $\epsilon \ll 1$. The oncoming flow is near sonic, $M_\infty \sim 1$, and is also characterized by small values of Γ, $\Gamma_\infty \sim 0$, and the second nonlinearity parameter $\Lambda = \rho(\partial\Gamma/\partial\rho)$, $\Lambda_\infty \sim 0$. The third nonlinearity parameter, $\Sigma = \rho^2(\partial^2\Gamma/\partial\rho^2)$, is considered of order of one, $\Sigma_\infty \sim O(1)$. They found significant increase of the critical Mach number in flows of BZT fluids over profiles. Numerical solutions revealed substantial reductions in the strength of compression shocks. A further benefit is an evident decrease of the drag that was found in the numerical study of Morren (1990) using the Euler equations and a van der Waals equation of state. These computations also revealed the formation of expansion shocks near the nose of the airfoil in regions where $\Gamma < 0$.

The pioneering work of Cramer and co-authors has constructed a framework for studying transonic flows of BZT fluids around airfoils. In the present paper we investigate the connections between the transonic small-disturbance theory of Tarkenton & Cramer (1993) and the numerical solutions of the Euler equations of Morren (1990). Of specific interest is the flow around the nose of the profile. In this region the flow changes significantly over a small area and those changes may affect the flow over the entire profile. One of the open problems to resolve is the appearance of sonic or supersonic shocks in the nose region. Theoretical work toward understanding the flow in the nose region can clarify this problem.

Despite being an important problem in the study of the aerodynamic properties of profiles, to the best of our knowledge the nature of the transonic flow of BZT fluids around the nose of a thin airfoil has never been addressed and is a great challenge to solve. The results may add to our understanding of the complicated physics of compressible flows of dense gases.

The present analysis follows the approach of Rusak (1993) for studying the transonic flow of a perfect gas around the nose of an airfoil. Asymptotic expansions of the velocity potential function are constructed in terms of the airfoil thickness ratio in an outer region around the airfoil and in an inner region near the nose. The outer expansion consists of the transonic small-disturbance theory for BZT gases, where a leading-edge singularity appears. Analytical expressions are given for this singularity by constructing similarity solutions of the governing nonlinear equation. The inner expansion accounts for the flow around the nose, where a stagnation point exists. A boundary value problem is formulated in the inner region for the solution of an oncoming uniform sonic flow with zero values of the fundamental derivative of gasdynamics and the second nonlinearity parameter around a parabola at zero

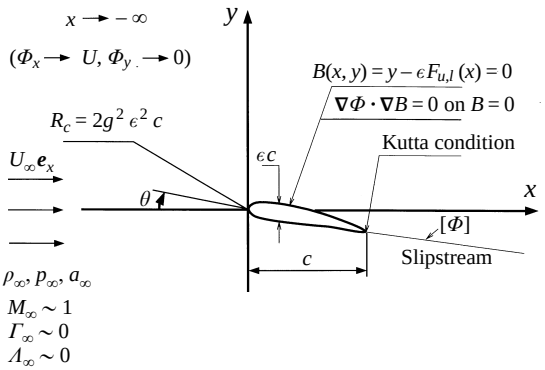

FIGURE 1. Airfoil problem.

angle of attack. The numerical solution of the inner problem results in a symmetric flow around the nose. The outer and inner expansions are matched asymptotically resulting in a uniformly valid composite solution around the entire airfoil. This composite solution is a good and relatively simple approximation to the solution of the Euler equations for the entire flow field. It is found that in the leading terms, the flow around the nose is symmetric and the stagnation point is located at the leading edge for every transonic Mach number, and small values of Γ and Λ of the oncoming flow and shape and small angle of attack of the airfoil.

2. Mathematical model

A steady inviscid flow around a two-dimensional thin airfoil with a parabolic nose is considered in an (x, y)-plane with unit vectors $(\boldsymbol{e}_x, \boldsymbol{e}_y)$ (figure 1). The flow far away ahead of the airfoil is assumed to be uniform at speed U_∞, density ρ_∞, entropy s_∞, speed of sound a_∞ and Mach number $M_\infty \equiv U_\infty/a_\infty \sim 1$. The oncoming flow is also characterized by small values of the fundamental derivative of gasdynamics ($\Gamma_\infty \sim 0$) and the second nonlinearity parameter ($\Lambda_\infty \sim 0$), and order of 1 of the third nonlinearity parameter ($\Sigma_\infty \sim O(1)$). The airfoil shape is given by

$$B(x, y) = y - \epsilon F_{u,l}(x) = 0 \quad \text{for} \quad 0 \leqslant x \leqslant c, \tag{1}$$

where c is the airfoil chord and ϵ is the thickness ratio, $\epsilon \ll 1$. The functions $F_{u,l}(x)$ represent the upper and lower surfaces, respectively. These shape functions are given by

$$F_{u,l}(x) = Ca(x) \pm c\ t(x/c) - \Theta x \quad \text{for} \quad 0 \leqslant x \leqslant c, \tag{2}$$

where $Ca(x)$ is the camber line function, $c\ t(x/c)$ is the thickness distribution, $\Theta = \theta/\epsilon$ and θ is the angle of attack. Also, $t(0) = t(1) = 0$ and $Ca(0) = Ca(c) = 0$. Near the leading edge as $x \to 0$ the thickness function changes like $c\ t(x/c) \sim 2g(cx)^{1/2} + O(x)$ and the camber line function changes like $Ca(x) \sim m_1 x + O(x^q)$ with $(q > 1)$. Here, $R_c = 2g^2\epsilon^2 c$ is the radius of curvature of the parabolic nose, g is a given constant and m_1 is the local camber of the airfoil at the leading edge (see Abbott & Doenhoff 1959, pp. 111–118).

The Rankine–Hugoniot relation in Thompson (1984) has been verified to be valid in our mathematical model. He found that the entropy rise and vorticity generated by shock waves in transonic flows is of fourth order in the shock strength whenever Γ is small. Therefore, to the orders of the disturbances in the pressure (p), density

(ρ) and velocity vector ($\boldsymbol{q}$) considered here, the flow may be taken as irrotational and isentropic, i.e. $s \sim s_\infty$ everywhere in the flow domain. The velocity potential field $\Phi(x, y)$ of the flow, where $\boldsymbol{q} = \nabla\Phi$, can be described by the full potential-flow equation:

$$(a^2 - \Phi_x^2)\Phi_{xx} - 2\Phi_x\Phi_y\Phi_{xy} + (a^2 - \Phi_y^2)\Phi_{yy} = 0 \tag{3}$$

and the Bernoulli equation,

$$h(\rho, s_\infty) + \tfrac{1}{2}\,|\nabla\Phi|^2 = h_\infty + \tfrac{1}{2}U_\infty^2. \tag{4}$$

Here, h is the enthalpy, $h_\infty = h(\rho_\infty, s_\infty)$, $a(\rho, s_\infty)$ is the thermodynamic speed of sound, $a^2 \equiv (\partial p/\partial\rho)_s^{1/2}$, and $p = p(\rho, s_\infty)$. The Bernoulli equation relates the disturbances in the speed of sound to those in Φ through the thermodynamic relations between a and h. The solution of (3) and (4) should satisfy the kinematic tangency boundary condition on the airfoil surface,

$$\nabla\Phi \cdot \nabla B = 0 \quad \text{on} \quad B = 0. \tag{5}$$

Also, disturbances must die out at upstream infinity, as $x \to -\infty$: $\Phi_x \to U_\infty$ and $\Phi_y \to 0$. The Kutta condition is satisfied at a sharp trailing edge. In order to get a one-valued potential function, the (x, y)-plane is cut along the slipstream that leaves the trailing edge to infinity and where the potential is allowed to jump due to the circulation around the airfoil.

Introducing the following non-dimensional variables:

$$\bar{x} = \frac{x}{c}, \qquad \bar{y} = \frac{y}{c}, \qquad \bar{\phi} = \frac{\Phi - U_\infty x}{U_\infty c}, \qquad \bar{a} = \frac{a}{a_\infty}, \qquad M_\infty^2 = \frac{U_\infty^2}{a_\infty^2} \tag{6}$$

the non-dimensional forms of (3)–(5) are given by

$$(M_\infty^2 + 2M_\infty^2\bar{\phi}_{\bar{x}} + M_\infty^2\bar{\phi}_{\bar{x}}^2 - \bar{a}^2)\bar{\phi}_{\bar{x}\bar{x}} + 2M_\infty^2(1 + \bar{\phi}_{\bar{x}})\bar{\phi}_{\bar{y}}\bar{\phi}_{\bar{x}\bar{y}} = (\bar{a}^2 - M_\infty^2\bar{\phi}_{\bar{y}}^2)\bar{\phi}_{\bar{y}\bar{y}} \tag{7}$$

and

$$\frac{h - h_\infty}{a_\infty^2} = -M_\infty^2\left(\bar{\phi}_{\bar{x}} + \frac{\bar{\phi}_{\bar{x}}^2 + \bar{\phi}_{\bar{y}}^2}{2}\right) \tag{8}$$

with

$$\bar{\phi}_{\bar{y}} = \epsilon(1 + \bar{\phi}_{\bar{x}})F'_{u,l}(\bar{x}) \quad \text{on} \quad \bar{y} = \epsilon F_{u,l}(\bar{x}) \quad \text{for} \quad 0 \leqslant \bar{x} \leqslant 1, \tag{9}$$

$$\bar{\phi}_{\bar{x}},\ \bar{\phi}_{\bar{y}} \to 0 \quad \text{as} \quad \bar{x} \to -\infty. \tag{10}$$

In order to study the transonic flow of BZT gases around a thin airfoil with a parabolic nose, the potential Φ is approximated by asymptotic expansions in the limit $\epsilon \to 0, M_\infty \to 1, \Gamma_\infty \to 0$ and $\Lambda_\infty \to 0$ and with the similarity parameters $K = (1 - M_\infty^2)/\epsilon^{6/5}, K_\Gamma = \Gamma_\infty/\epsilon^{4/5}, K_\Lambda = \Lambda_\infty/\epsilon^{2/5}$ and Σ_∞ fixed. An outer expansion is constructed in an outer region around the airfoil. There the coordinates $(\bar{x}, \tilde{y} = \epsilon^{3/5}\bar{y})$ are fixed as $\epsilon \to 0$. An inner expansion is constructed in the nose region using stretched coordinates. There the coordinates $(x^* = \bar{x}/\epsilon^2, y^* = \bar{y}/\epsilon^2)$ are fixed as $\epsilon \to 0$. The various powers in these expansions result from the following asymptotic analysis (see also Cramer & Tarkenton 1992; Tarkenton & Cramer 1993; Kluwick 1993).

3. Outer expansion

3.1. *Small-disturbance theory*

In the outer region around the airfoil, we consider the limit $\epsilon \to 0, M_\infty \to 1$, $\Gamma_\infty \to 0, \Lambda_\infty \to 0$, where

$$M_\infty^2 = 1 - K\mu(\epsilon), \quad \Gamma_\infty = K_\Gamma \gamma(\epsilon) + \ldots, \quad \Lambda_\infty = K_\Lambda \lambda(\epsilon) + \ldots \tag{11}$$

and $(\bar{x}, \tilde{y} = \beta(\epsilon)\bar{y}; K, K_\Gamma, K_\Lambda, \Sigma_\infty, \Theta)$ fixed. Here, $\mu \ll 1, \gamma \ll 1, \lambda \ll 1$ and $\beta \ll 1$. In this region, we expect that the flow disturbances created by the airfoil are relatively small compared to the uniform-stream properties. Therefore, the potential and the density in the outer region may be approximated by the asymptotic expansions:

$$\begin{aligned} \Phi = U_\infty c\{&\bar{x} + \delta_1(\epsilon)\bar{\phi}_1(\bar{x}, \tilde{y}; K, K_\Gamma, K_\Lambda, \Sigma_\infty, \Theta) \\ &+\delta_2(\epsilon)\bar{\phi}_2(\bar{x}, \tilde{y}; K, K_\Gamma, K_\Lambda, \Sigma_\infty, \Theta) \\ &+\delta_3(\epsilon)\bar{\phi}_3(\bar{x}, \tilde{y}; K, K_\Gamma, K_\Lambda, \Sigma_\infty, \Theta) + \ldots\}, \end{aligned} \tag{12}$$

$$\rho = \rho_\infty + l_1(\epsilon)\rho_1 + l_2(\epsilon)\rho_2 + l_3(\epsilon)\rho_3 + \ldots. \tag{13}$$

Here, $\delta_3 \ll \delta_2 \ll \delta_1 \ll 1$, and $l_3 \ll l_2 \ll l_1 \ll 1$. Because $h = h(\rho, s)$, the Taylor series expansion of h may be given by

$$\begin{aligned} h(\rho, s = s_\infty) = h_\infty &+ \left.\frac{\partial h}{\partial \rho}\right|_{(\rho_\infty, s_\infty)} (l_1(\epsilon)\rho_1 + l_2(\epsilon)\rho_2 + l_3(\epsilon)\rho_3 + \ldots) \\ &+ \frac{1}{2}\left.\frac{\partial^2 h}{\partial \rho^2}\right|_{(\rho_\infty, s_\infty)} (l_1(\epsilon)\rho_1 + l_2(\epsilon)\rho_2 + \ldots)^2 + \frac{1}{6}\left.\frac{\partial^3 h}{\partial \rho^3}\right|_{(\rho_\infty, s_\infty)} (l_1(\epsilon)\rho_1 + \ldots)^3 + \ldots. \end{aligned} \tag{14}$$

From the Gibbs' equation,

$$\mathrm{d}h = T\,\mathrm{d}s + \frac{\mathrm{d}p}{\rho}, \tag{15}$$

the definition of Γ, and (11), since to the orders considered $\mathrm{d}s \sim 0$, we have

$$\left.\frac{\partial h}{\partial \rho}\right|_{(\rho_\infty, s_\infty)} = \frac{a_\infty^2}{\rho_\infty}, \quad \left.\frac{\partial^2 h}{\partial \rho^2}\right|_{(\rho_\infty, s_\infty)} = -3\frac{a_\infty^2}{\rho_\infty^2} + O(\gamma(\epsilon)), \quad \left.\frac{\partial^3 h}{\partial \rho^3}\right|_{(\rho_\infty, s_\infty)} = 12\frac{a_\infty^2}{\rho_\infty^3} + O(\gamma(\epsilon)). \tag{16}$$

Therefore, with the assumption that $l_1^2\gamma \ll l_3$ (this will be proved in the next paragraph), we get

$$\frac{h - h_\infty}{a_\infty^2} = l_1(\epsilon)\frac{\rho_1}{\rho_\infty} + l_2(\epsilon)\left(\frac{\rho_2}{\rho_\infty} - \frac{3}{2}\frac{\rho_1^2}{\rho_\infty^2}\right) + l_3(\epsilon)\left(\frac{\rho_3}{\rho_\infty} - 3\frac{\rho_1\rho_2}{\rho_\infty^2} + 2\frac{\rho_1^3}{\rho_\infty^3}\right) + \ldots. \tag{17}$$

Equation (17) shows that to the leading order, the enthalpy disturbance can be approximated by the density disturbance. From (12) and (17), the Bernoulli equation (8) becomes

$$\begin{aligned} l_1(\epsilon)\left(\frac{\rho_1}{\rho_\infty}\right) &+ l_2(\epsilon)\left(\frac{\rho_2}{\rho_\infty} - \frac{3}{2}\frac{\rho_1^2}{\rho_\infty^2}\right) + l_3(\epsilon)\left(\frac{\rho_3}{\rho_\infty} - 3\frac{\rho_1\rho_2}{\rho_\infty^2} + 2\frac{\rho_1^3}{\rho_\infty^3}\right) + \ldots \\ &= \delta_1(\epsilon)\left(-\bar{\phi}_{1\bar{x}}\right) + \delta_1(\epsilon)\mu(\epsilon)\left(K\bar{\phi}_{1\bar{x}}\right) + \delta_2(\epsilon)\left(-\bar{\phi}_{2\bar{x}} - \tfrac{1}{2}\bar{\phi}_{1\bar{x}}^2\right) \\ &\quad +\delta_2(\epsilon)\mu(\epsilon)\left(K\bar{\phi}_{2\bar{x}} + \tfrac{1}{2}K\bar{\phi}_{1\bar{x}}^2\right) + \delta_3(\epsilon)\left(-\bar{\phi}_{3\bar{x}} - \bar{\phi}_{1\bar{x}}\bar{\phi}_{2\bar{x}}\right) + \ldots. \end{aligned} \tag{18}$$

We find that $l_1(\epsilon) = \delta_1(\epsilon)$, $l_2(\epsilon) = \delta_2(\epsilon) = l_1^2(\epsilon)$, $l_3(\epsilon) = \delta_3(\epsilon) = l_1^3(\epsilon)$ and

$$\frac{\rho_1}{\rho_\infty} = -\bar{\phi}_{1\bar{x}}, \quad \frac{\rho_2}{\rho_\infty} = -\bar{\phi}_{2\bar{x}} + \bar{\phi}_{1\bar{x}}^2, \quad \frac{\rho_3}{\rho_\infty} = -\bar{\phi}_{3\bar{x}} + 2\bar{\phi}_{1\bar{x}}\bar{\phi}_{2\bar{x}} - \bar{\phi}_{1\bar{x}}^3. \tag{19}$$

Here, we also assume that $\delta_1\mu \ll \delta_3$ (this will be proved in the following paragraph). Equation (19) shows that to the leading order, the density and enthalpy disturbances can be approximated from the axial velocity disturbance. Because $a = a(\rho, s)$, the Taylor series expansion of a may be given by

$$a^2(\rho, s = s_\infty) = a_\infty^2 + \left.\frac{\partial(a^2)}{\partial\rho}\right|_{(\rho_\infty, s_\infty)} (l_1(\epsilon)\rho_1 + l_2(\epsilon)\rho_2 + l_3(\epsilon)\rho_3 + \ldots)$$
$$+\frac{1}{2}\left.\frac{\partial^2(a^2)}{\partial\rho^2}\right|_{(\rho_\infty, s_\infty)} (l_1(\epsilon)\rho_1 + l_2(\epsilon)\rho_2 + \ldots)^2 + \frac{1}{6}\left.\frac{\partial^3(a^2)}{\partial\rho^3}\right|_{(\rho_\infty, s_\infty)} (l_1(\epsilon)\rho_1 + \ldots)^3 + \ldots. \quad (20)$$

From the expansions of Γ_∞, Λ_∞ in (11) and the definition of Σ_∞, we have

$$\left.\frac{\partial(a^2)}{\partial\rho}\right|_{(\rho_\infty, s_\infty)} = 2\frac{a_\infty^2}{\rho_\infty}(-1 + K_\Gamma\gamma(\epsilon)), \quad (21a)$$

$$\left.\frac{\partial^2(a^2)}{\partial\rho^2}\right|_{(\rho_\infty, s_\infty)} = \frac{a_\infty^2}{\rho_\infty^2}(6 + 2(K_\Gamma\gamma(\epsilon))^2 - 6K_\Gamma\gamma(\epsilon) + 2K_\Lambda\lambda(\epsilon)), \quad (21b)$$

$$\left.\frac{\partial^3(a^2)}{\partial\rho^3}\right|_{(\rho_\infty, s_\infty)} = \frac{a_\infty^2}{\rho_\infty^3}(-24 + 2\Sigma_\infty + 8K_\Gamma K_\Lambda\gamma(\epsilon)\lambda(\epsilon)$$
$$-14K_\Lambda\lambda(\epsilon) - 6(K_\Gamma\gamma(\epsilon))^2 + 24K_\Gamma\gamma(\epsilon)). \quad (21c)$$

From (19)–(21) and (7), we can show after some algebra that

$$\left\{-K\mu(\epsilon) + \delta_1(\epsilon)\gamma(\epsilon)2K_\Gamma\bar{\phi}_{1\bar{x}} - \delta_1^2(\epsilon)\lambda(\epsilon)K_\Lambda\bar{\phi}_{1\bar{x}}^2 + \delta_1^3(\epsilon)\tfrac{1}{3}\Sigma_\infty\bar{\phi}_{1\bar{x}}^3\right\}\delta_1(\epsilon)\bar{\phi}_{1\bar{x}\bar{x}} + \ldots$$
$$= \delta_1(\epsilon)\beta^2(\epsilon)\bar{\phi}_{1\tilde{y}\tilde{y}} + \ldots. \quad (22)$$

Therefore, through matching the disturbance scales, we find $\mu(\epsilon) = \delta_1^3(\epsilon) = \delta_1(\epsilon)\gamma(\epsilon) = \delta_1^2(\epsilon)\lambda(\epsilon) = \beta^2(\epsilon)$. Now, from the boundary condition (9), we have $\delta_1(\epsilon)\beta(\epsilon) = \epsilon$. As a result, we have $\delta_1(\epsilon) = l_1(\epsilon) = \epsilon^{2/5}$, $\beta(\epsilon) = \epsilon^{3/5}$, $\mu(\epsilon) = \epsilon^{6/5}$, $\gamma(\epsilon) = \epsilon^{4/5}$, $\lambda(\epsilon) = \epsilon^{2/5}$ (these also prove the assumptions made above) and

$$\left.\begin{array}{c}\tilde{y} = \epsilon^{3/5}\bar{y},\ M_\infty^2 = 1 - \epsilon^{6/5}K,\ \Gamma_\infty = \epsilon^{4/5}K_\Gamma + \ldots,\ \Lambda_\infty = \epsilon^{2/5}K_\Lambda + \ldots,\\ \Phi = U_\infty c\left\{\bar{x} + \epsilon^{2/5}\bar{\phi}_1(\bar{x}, \tilde{y}; K, K_\Gamma, K_\Lambda, \Sigma_\infty, \Theta) + O(\epsilon^{4/5})\right\}.\end{array}\right\} \quad (23)$$

Here the perturbation function $\bar{\phi}_1$ is described by

$$\left(-K + 2K_\Gamma\bar{\phi}_{1\bar{x}} - K_\Lambda\bar{\phi}_{1\bar{x}}^2 + \tfrac{1}{3}\Sigma_\infty\bar{\phi}_{1\bar{x}}^3\right)\bar{\phi}_{1\bar{x}\bar{x}} = \bar{\phi}_{1\tilde{y}\tilde{y}}. \quad (24)$$

This equation is a modified Kármán–Guderley equation for transonic flows of the BZT gases and an equivalent version of this equation was previously derived by Kluwick (1993) and Tarkenton & Cramer (1993) in their transonic small-disturbance theory for BZT gases. The function $\bar{\phi}_1$ should satisfy the following boundary conditions:

$$\left.\begin{array}{rl}\bar{\phi}_{1\tilde{y}}(\bar{x}, 0\pm) = F'_{u,l}(\bar{x}) & \text{for}\quad 0 \leqslant \bar{x} \leqslant 1,\\ \bar{\phi}_{1\bar{x}}, \bar{\phi}_{1\tilde{y}} \to 0 & \text{as}\quad \bar{x} \to -\infty.\end{array}\right\} \quad (25)$$

We can also show that under the above approximations the pressure field may be given by the axial velocity disturbances, $p = p_\infty(\rho_\infty, s_\infty) - \rho_\infty a_\infty^2\epsilon^{2/5}\bar{\phi}_{1\bar{x}} + \ldots$ and the pressure coefficient by $c_p = (p - p_\infty)/(\frac{1}{2}\rho_\infty U_\infty^2) = -2\epsilon^{2/5}\bar{\phi}_{1\bar{x}} + \ldots$. Therefore, the Kutta condition at the airfoil's trailing edge results in

$$\bar{\phi}_{1\bar{x}}(1, 0^+) = \bar{\phi}_{1\bar{x}}(1, 0^-). \quad (26)$$

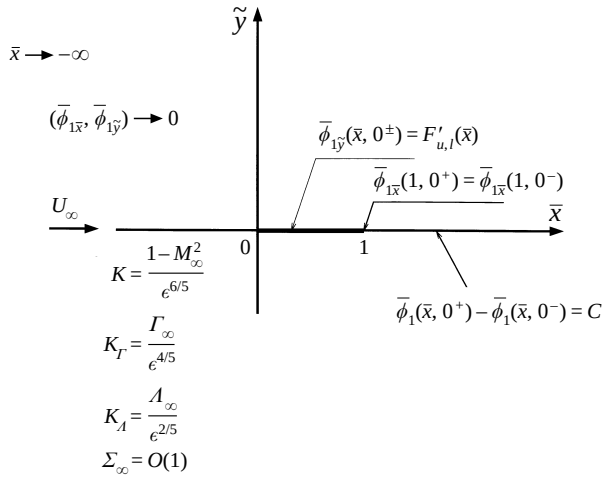

FIGURE 2. Transonic small-disturbance problem.

Also, to get a one-valued potential function $\bar{\phi}_1$, we have $\bar{\phi}_1(\bar{x}, 0^+) - \bar{\phi}_1(\bar{x}, 0^-) = C$ for every $\bar{x} \geqslant 1$, where C is the circulation around the airfoil (see figure 2). The fundamental derivative of gasdynamics can also be estimated from the axial velocity disturbance according to the small-disturbance theory: $\Gamma = \epsilon^{4/5}(K_\Gamma - K_\Lambda \bar{\phi}_{1\bar{x}}) + \ldots$.

3.2. *Nose singularity*

In this subsection, we study the flow near the airfoil's parabolic nose according to the small-disturbance theory. The solution of (24)–(26) in the nose region (as $(\bar{x}, \tilde{y}) \to 0$) is approximated by the sum of similarity terms,

$$E^{1/3}\bar{\phi}_1 = \tilde{y}^m f(\xi) + \ldots, \quad \xi = \frac{\bar{x}}{\tilde{y}^k} \tag{27}$$

where $E = \Sigma_\infty/3 > 0$ and k, m are constants and f is the similarity function. From (24) and (27), it is found that in the leading order the effects of the terms $K\bar{\phi}_{1\bar{x}\bar{x}}$, $K_\Gamma \bar{\phi}_{1\bar{x}}\bar{\phi}_{1\bar{x}\bar{x}}$ and $K_\Lambda \bar{\phi}_{1\bar{x}}^2\bar{\phi}_{1\bar{x}\bar{x}}$ are smaller than the effect of $E\bar{\phi}_{1\bar{x}}^3\bar{\phi}_{1\bar{x}\bar{x}}$. Therefore, $m = \frac{1}{3}(5k-2)$ and $f(\xi)$ is described by the nonlinear differential equation

$$(f_\xi^3 - k^2\xi^2)f_{\xi\xi} - \tfrac{7}{3}k(1-k)\xi f_\xi + \tfrac{5}{9}(1-k)(5k-2)f = 0. \tag{28}$$

From (27), the approximation of $\bar{\phi}_{1\tilde{y}}$ as $\tilde{y} \to 0\pm$ and $\bar{x} > 0$ (as $\xi \to +\infty$) gives

$$\bar{\phi}_{1\tilde{y}}(\bar{x}, 0\pm) = E^{-1/3}\bar{x}^{5(k-1)/3k}\xi^{3k/[5(k-1)]}\left[\tfrac{1}{3}(5k-2)f - k\xi f_\xi\right] \tag{29}$$

and from the boundary condition (25) and the assumptions on the airfoil shape near the leading edge, we find that $5(k-1)/3k = -1/2$, or $k = 10/13$ and $m = 8/13$. Therefore,

$$E^{1/3}\bar{\phi}_1 = \tilde{y}^{8/13}f(\xi) + \ldots, \quad \xi = \frac{\bar{x}}{\tilde{y}^{10/13}} \tag{30}$$

and from (28)

$$(f_\xi^3 - \tfrac{100}{169}\xi^2)f_{\xi\xi} - \tfrac{70}{169}\xi f_\xi + \tfrac{40}{169}f = 0. \tag{31}$$

In order to solve (31), the following hodograph analysis is used. As the local flow near the airfoil leading edge approaches stagnation, (24) may be reduced to

$$E\bar{\phi}_{1\bar{x}}^3\bar{\phi}_{1\bar{x}\bar{x}} - \bar{\phi}_{1\tilde{y}\tilde{y}} = 0 \tag{32}$$

which also describes a sonic small-disturbance flow with $K = K_\Gamma = K_A = 0$. Let

$$w \equiv E^{1/3}\bar{\phi}_{1\bar{x}},\ v \equiv E^{1/3}\bar{\phi}_{1\tilde{y}}$$

then, (32) is equivalent to the modified Kármán–Guderley system:

$$w^3 w_{\bar{x}} - v_{\tilde{y}} = 0, \quad w_{\tilde{y}} - v_{\bar{x}} = 0. \tag{33}$$

The transformation from the transonic plane, $(w(\bar{x},\tilde{y}), v(\bar{x},\tilde{y}))$, to the hodograph plane, $(\bar{x}(w,v), \tilde{y}(w,v))$, results in a modified Tricomi system:

$$w^3\tilde{y}_v - \bar{x}_w = 0, \quad \bar{x}_v - \tilde{y}_w = 0 \tag{34}$$

or in the modified Tricomi equation: $w^3\tilde{y}_{vv} - \tilde{y}_{ww} = 0$. We define the variables

$$\tau \equiv \tfrac{2}{5}(-w)^{5/2} \tag{35}$$

and (r,α) through

$$\tau = r\cos\alpha > 0\ , \quad v = r\sin\alpha, \quad -\tfrac{1}{2}\pi < \alpha < \tfrac{1}{2}\pi. \tag{36}$$

The system (34) becomes

$$\bar{x}_r = \left(\tfrac{5}{2}\right)^{3/5} r^{-2/5}(\cos^{3/5}\alpha)\tilde{y}_\alpha, \quad \bar{x}_\alpha = -\left(\tfrac{5}{2}\right)^{3/5} r^{8/5}(\cos^{3/5}\alpha)\tilde{y}_r. \tag{37}$$

Equation (37) may be reduced to

$$\tilde{y}_{rr} + \frac{8}{5r}\tilde{y}_r + \frac{1}{r^2}\tilde{y}_{\alpha\alpha} - \frac{3}{5r^2}(\tan\alpha)\tilde{y}_\alpha = 0. \tag{38}$$

For solving $\tilde{y}$, we suggest the separation-of-variables solution

$$\tilde{y} = R(r)A(\alpha) \tag{39}$$

where the functions $R(r)$ and $A(\alpha)$ are described by

$$r^2R'' + \tfrac{8}{5}rR' - \nu^2 R = 0, \quad A'' - \tfrac{3}{5}(\tan\alpha)A' + \nu^2 A = 0. \tag{40}$$

Here, ν is a constant to be determined. Let $R = r^d$, then $d(d-1) + \frac{8}{5}d - \nu^2 = 0$ and $d = -\frac{3}{10} \pm \eta$, where $\eta = (\frac{9}{100} + \nu^2)^{1/2}$. Since we look for a nose singularity, $R \to \infty$ as $r \to 0$, the only valid solution is

$$R = r^{-3/10-\eta}. \tag{41}$$

For solving $A(\alpha)$, let $z = \sin^2\alpha = (v/r)^2$. Then from (40), we have

$$z(1-z)A_{zz} + \left(\tfrac{1}{2} - \tfrac{13}{10}z\right)A_z + \tfrac{1}{4}\nu^2 A = 0. \tag{42}$$

This is the standard hypergeometric equation (Abramowitz & Stegun 1965), the solution of which is given by

$$A(\alpha) = c_1 \sin\alpha\ F_1 + c_2\ F_2 \tag{43}$$

where

$$F_1 = F\left(\tfrac{13}{20} + \tfrac{1}{2}\eta, \tfrac{13}{20} - \tfrac{1}{2}\eta; \tfrac{3}{2}; \sin^2\alpha\right),$$

$$F_2 = F\left(\tfrac{3}{20} + \tfrac{1}{2}\eta, \tfrac{3}{20} - \tfrac{1}{2}\eta; \tfrac{1}{2}; \sin^2\alpha\right)$$

and $c_1,\ c_2$ are constants to be determined. So,

$$\tilde{y} = R(r)A(\alpha) = c_1\ r^{-3/10-\eta}(\sin\alpha\ F_1 + \tilde{c}_2\ F_2) \tag{44}$$

where $\tilde{c}_2 = c_2/c_1$. Now, from (27), we have

$$\left.\begin{aligned} w &= E^{1/3}\bar{\phi}_{1\bar{x}} = \tilde{y}^{m-k} f_\xi = \tilde{y}^{2(k-1)/3} f_\xi, \\ v &= E^{1/3}\bar{\phi}_{1\tilde{y}} = \tilde{y}^{m-1}\left(mf - k\xi f_\xi\right) = \tilde{y}^{5(k-1)/3}\left[\tfrac{1}{3}(5k-2)f - k\xi f_\xi\right] \end{aligned}\right\} \tag{45}$$

and $r = \tilde{y}^{5(k-1)/3} f_{n1}(\xi)$, $\tan\alpha = f_{n2}(\xi)$ where the functions $f_{n1}(\xi)$, $f_{n2}(\xi)$ are related to f and f_ξ. Therefore, we find that

$$\tilde{y} = r^{3/[5(k-1)]}\bar{f}_{n1}(\alpha), \quad \xi = \bar{f}_{n2}(\alpha). \tag{46}$$

Here, $\bar{f}_{n1}$ and $\bar{f}_{n2}$ are the inverse functions of f_{n1} and f_{n2} respectively. The comparison between (44) and (46) gives $-\frac{3}{10} - \eta = 3/[5(k-1)]$. For the given airfoil, since $k = 10/13$, we have $\eta = 23/10$ and $v^2 = 26/5$. Therefore,

$$\left.\begin{aligned} \tilde{y} &= c_1\, r^{-13/5}\tilde{A}(\alpha), \\ \tilde{A}(\alpha) &= \sin\alpha\, F\left(\tfrac{9}{5}, -\tfrac{1}{2}; \tfrac{3}{2}; \sin^2\alpha\right) + \tilde{c}_2 F\left(\tfrac{13}{10}, -1; \tfrac{1}{2}; \sin^2\alpha\right). \end{aligned}\right\} \tag{47}$$

From the solution for $\tilde{y}$ and (37), we can integrate $\bar{x}$:

$$\bar{x} = -\tfrac{1}{2}\left(\tfrac{5}{2}\right)^{3/5} c_1\, r^{-2}\cos^{8/5}\alpha\, \frac{\mathrm{d}\tilde{A}(\alpha)}{\mathrm{d}(\sin\alpha)} \tag{48}$$

where

$$\frac{\mathrm{d}\tilde{A}(\alpha)}{\mathrm{d}(\sin\alpha)} = F\left(\tfrac{9}{5}, -\tfrac{1}{2}; \tfrac{1}{2}; \sin^2\alpha\right) - \tfrac{26}{5}\tilde{c}_2 \sin\alpha. \tag{49}$$

From (30), (47) and (48), we have a solution for $\xi(\alpha)$:

$$\xi(\alpha) = -\frac{\left(\frac{5}{2}\right)^{3/5} c_1^{3/13}\ \cos^{8/5}\alpha\ \mathrm{d}\tilde{A}(\alpha)/\mathrm{d}(\sin\alpha)}{2(\tilde{A}(\alpha))^{10/13}}. \tag{50}$$

Also, from (45) we find

$$f = \frac{3}{5k-2}\left(v\tilde{y}^{5(1-k)/3} + k\xi w\tilde{y}^{2(1-k)/3}\right) \tag{51}$$

and using (35), (36), (47) and (50), we find the solutions for $f(\alpha)$,

$$f(\alpha) = \tfrac{13}{8}c_1^{5/13}\ \frac{\sin\alpha\ \tilde{A}(\alpha) + \frac{25}{26}\cos^2\alpha\ \mathrm{d}\tilde{A}(\alpha)/\mathrm{d}(\sin\alpha)}{(\tilde{A}(\alpha))^{8/13}} \tag{52}$$

and $f_\xi(\alpha)$,

$$f_\xi = -(\tfrac{5}{2})^{2/5} c_1^{2/13}\ \tilde{A}^{2/13}(\alpha)\cos^{2/5}\alpha. \tag{53}$$

Equations (50) and (52) give an exact analytical solution of (31) and define a parametric representation of the similarity function $f(\xi)$ in terms of the hodograph similarity variable α. It should be noted that the constants c_1 and $\tilde{c}_2$ that appear in $A(\alpha)$ are yet to be determined.

The solution $\tilde{y}$ in (47) is given by a linear combination of symmetric and unsymmetric functions, in terms of the hodograph similarity variable α (see figure 3). The parameter α is determined in the range $\alpha_1 \leqslant \alpha \leqslant \alpha_3$, where $\alpha_1 < 0$, α_2, and $\alpha_3 > 0$ are the first three roots around $\alpha = 0$ of the equation $\tilde{y} = 0$ or $\tilde{A}(\alpha) = 0$. It is clear that the three roots are functions of $\tilde{c}_2$ only. In the hodograph plane the lines $\alpha = \alpha_1$ and $\alpha = \alpha_3$ represent the boundary curves of the lower and upper surfaces of the airfoil as $\bar{x} \to 0$. The third (intermediate) root, $\alpha = \alpha_2$, represents the $\bar{x}$-axis ahead of the airfoil.

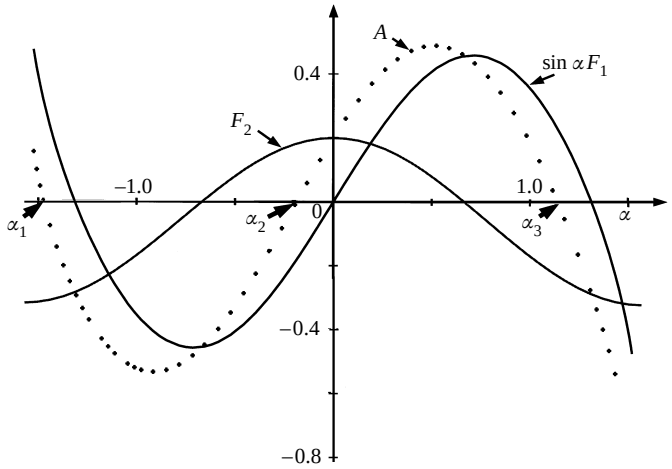

FIGURE 3. Mathematical diagram of function $A(\alpha)$ vs. α.

The substitution of (30), (50), (52) and (53) into (45) results in the velocity perturbations in the leading-edge region

$$w = -(\tfrac{5}{2})^{2/5} c_1^{2/13} \tilde{y}^{-2/13}\ \tilde{A}^{2/13}(\alpha)\ \cos^{2/5}\alpha$$
$$= -\left(\frac{c_1}{\bar{x}}\right)^{1/5} (\tfrac{1}{2})^{1/5} (\tfrac{5}{2})^{13/25} \left[\cos^{18/25}\alpha \left(-\frac{\mathrm{d}\tilde{A}(\alpha)}{\mathrm{d}(\sin\alpha)}\right)^{1/5}\right], \tag{54a}$$

$$v = c_1^{5/13} \tilde{y}^{-5/13}\ \tilde{A}^{5/13}(\alpha)\ \sin\alpha = \left(\frac{c_1}{\bar{x}}\right)^{1/2} (\tfrac{1}{2})^{1/2} (\tfrac{5}{2})^{3/10} \left[\sin\alpha\ \cos^{4/5}\alpha \left(-\frac{\mathrm{d}\tilde{A}(\alpha)}{\mathrm{d}(\sin\alpha)}\right)^{1/2}\right]. \tag{54b}$$

As $\tilde{y} \to 0\pm$ and $x > 0$ (as $\xi \to \infty$) then $\alpha \to \alpha_{1,3}(\tilde{c}_2)$. From the wing shape near the leading edge, equations (25) and (54*b*) give

$$v(\bar{x}, 0\pm) = \left(\frac{c_1}{\bar{x}}\right)^{1/2} (\tfrac{1}{2})^{1/2} (\tfrac{5}{2})^{3/10} \left[\sin\alpha\ \cos^{4/5}\alpha \left(-\frac{\mathrm{d}\tilde{A}(\alpha)}{\mathrm{d}(\sin\alpha)}\right)^{1/2}\right]_{\alpha\to\alpha_{1,3}(\tilde{c}_2)} + \ldots$$
$$= E^{1/3} g \left(\frac{c}{\bar{x}}\right)^{1/2} + \ldots. \tag{55}$$

Therefore,

$$c_1 = 2E^{2/3} \left(\tfrac{2}{5}\right)^{3/5} \frac{g^2 c}{\left[\sin^2\alpha\ \cos^{8/5}\alpha \left(-\mathrm{d}\tilde{A}(\alpha)/\mathrm{d}(\sin\alpha)\right)\right]_{\alpha\to\alpha_{1,3}(\tilde{c}_2)}}. \tag{56}$$

It can be shown that

$$\left[-\frac{\mathrm{d}\tilde{A}(\alpha)}{\mathrm{d}(\sin\alpha)}\right]_{\alpha\to\alpha_{1,3}(\tilde{c}_2)} = \left[\frac{1}{\cos^{8/5}\alpha \left(\frac{13}{5}\sin^2\alpha - 1\right)}\right]_{\alpha=\alpha_{1,3}(\tilde{c}_2)} \tag{57}$$

and so,

$$c_1 = 2E^{2/3} \left(\tfrac{2}{5}\right)^{3/5} g^2 c \left(\frac{13}{5} - \frac{1}{\sin^2\alpha}\right)_{\alpha=\alpha_{1,3}(\tilde{c}_2)}. \tag{58}$$

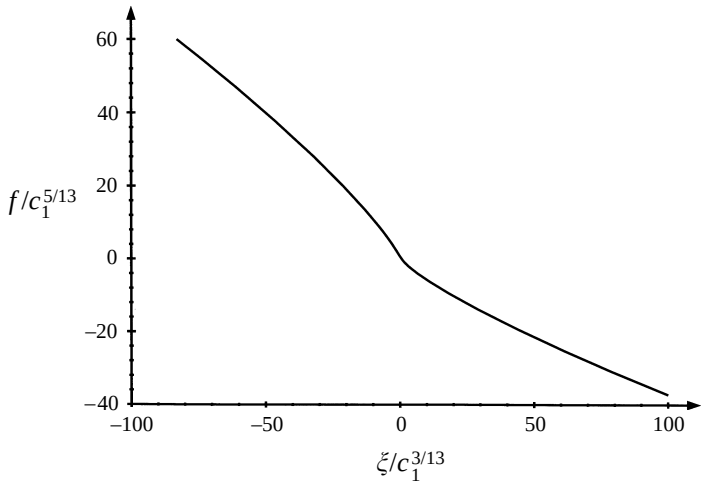

FIGURE 4. First-order similarity function $f(\xi)$.

Since $\alpha_1(\tilde{c}_2) \neq \alpha_2(\tilde{c}_2)$ for any $c_2 \neq 0$ and the solution has to be continuous across the $(\bar{x} < 0)$ axis as $\tilde{y} \to 0\pm$, it is found that the tangency boundary condition (25) or (55) can be satisfied consistently if and only if $\tilde{c}_2 = 0$. This means that

$$\tilde{A}(\alpha) = \sin\alpha \; F\left(\tfrac{9}{5}, -\tfrac{1}{2}; \tfrac{3}{2}; \sin^2\alpha\right) \tag{59}$$

where $-\alpha_3 \leqslant \alpha \leqslant \alpha_3$ and α_3 is the solution of the equation $F\left(\frac{9}{5}, -\frac{1}{2}; \frac{3}{2}; \sin^2\alpha\right) = 0$, $\alpha_3 = 75.383226^\circ$ and $\alpha_2 = 0$. In summary, the leading term of the transonic small-disturbance flow around the parabolic nose is given by

$$\left.\begin{aligned} E^{1/3}\bar{\phi}_1 &= \tilde{y}^{8/13} f(\xi) + \ldots, \\ \xi(\alpha) &= -\tfrac{1}{2}\left(\tfrac{5}{2}\right)^{3/5} c_1^{3/13} \frac{\cos^{8/5}\alpha \; F(\frac{9}{5}, -\frac{1}{2}; \frac{1}{2}; \sin^2\alpha)}{\sin^{10/13}\alpha \; F^{10/13}(\frac{9}{5}, -\frac{1}{2}; \frac{3}{2}; \sin^2\alpha)}, \\ f(\alpha) &= c_1^{5/13} \; \frac{26\sin^2\alpha F(\frac{9}{5}, -\frac{1}{2}; \frac{3}{2}; \sin^2\alpha) + 25\cos^2\alpha \; F(\frac{9}{5}, -\frac{1}{2}; \frac{1}{2}; \sin^2\alpha)}{16[\sin\alpha \; F(\frac{9}{5}, -\frac{1}{2}; \frac{3}{2}; \sin^2\alpha)]^{8/13}}, \end{aligned}\right\} \tag{60}$$

where $c_1 = 1.768163 g^2 c$. The function $f(\xi)$ is described in figure 4. It is a monotonically decreasing function. This flow is symmetric about the $\bar{x}$-axis.

From (45), (54), (57) and (58), we can calculate the distribution of c_p and Γ, on the airfoil surface and near leading edge, from the transonic small-disturbance theory for BZT gases,

$$\left.\begin{aligned} c_p &\sim 2\epsilon^{2/5}\left(\tfrac{5}{2}\right)^{2/5} E^{-1/5}(g^2 c)^{1/5}\cot^{2/5}\alpha_3 \; x^{-1/5} + \ldots \\ &= 1.685483 E^{-1/5}(\epsilon^2 g^2 c)^{1/5} \; x^{-1/5} + \ldots, \\ \Gamma &\sim \epsilon^{4/5}\left(K_\Gamma + K_\Lambda\left(\tfrac{5}{2}\right)^{2/5} E^{-1/5}(g^2 c)^{1/5}\cot^{2/5}\alpha_3 \; x^{-1/5} + \ldots\right) + \ldots \\ &= \epsilon^{4/5}\left(K_\Gamma + 0.842742 K_\Lambda E^{-1/5}(g^2 c)^{1/5} \; x^{-1/5} + \ldots\right). \end{aligned}\right\} \tag{61}$$

We can see that on the airfoil surface, both the pressure and the fundamental derivative of gasdynamics are symmetric near the leading edge and independent of the angle of attack. Also, both parameters have a leading-edge singularity and describe a subsonic flow with no shocks in the vicinity of the leading edge.

The results can be summarized as follows. From (12) and (60), the potential Φ in the outer region can be approximated in the leading-edge region as ($\epsilon \to 0, M_\infty \to 1, \Gamma_\infty \to 0, \Lambda_\infty \to 0$), with ($\bar{x}, \tilde{y}; K, K_\Gamma, K_\Lambda, \Sigma_\infty, \Theta$) fixed, by the asymptotic expansion

$$\Phi \sim U_\infty c \left\{ \bar{x} + \frac{\epsilon^{2/5}}{E^{1/3}} \tilde{y}^{8/13} f(\xi) + \ldots \right\} \tag{62}$$

where $\xi = \bar{x}/\tilde{y}^{10/13}$. Equation (62) shows that in the leading-edge region as both $\bar{x}$ and $\tilde{y}$ tend to zero, the velocities in the $\bar{x}$- and $\tilde{y}$-directions, as well as the pressure and Γ, become singular, specifically on the airfoil surface. This singularity implies that the disturbances from the uniform flow properties become relatively large near the nose of the airfoil. Therefore, the transonic small-disturbance theory cannot properly represent the flow in this region.

There is also a misordering in the approximation (62) in the magnitude of the disturbance for every ξ when both $\bar{x}$ and $\bar{y}$ are smaller than $\epsilon^2 g^2 c$. Therefore, a rescaling in the radial direction only is needed, $x^* = \bar{x}/\epsilon^2, y^* = \bar{y}/\epsilon^2$, to account for the local flow around the airfoil nose, where a stagnation point exits.

4. Inner expansion

In the inner region, around the parabolic nose of the airfoil, we expect that the flow disturbances created by the airfoil are relatively large compared to the uniform-stream properties. Therefore, the asymptotic expansion of the potential Φ is given in the limit ($\epsilon \to 0, M_\infty \to 1, \Gamma_\infty \to 0, \Lambda_\infty \to 0$), with ($x^*, y^*; K, K_\Gamma, K_\Lambda, \Sigma_\infty, \Theta$) fixed, in the form of

$$\Phi(x, y) = U_\infty c\, \epsilon^2 \left(x^* + \phi_0 \left(x^*, y^* \right) \right) + \ldots. \tag{63}$$

Here, we expect that $\phi_0 (x^*, y^*)$ describes large variations. From (3), (4) and (63), we have the governing equation

$$\left(\frac{a^2}{U_\infty^2} - (1 + \phi_{0x^*})^2 \right) \phi_{0x^*x^*} - 2(1 + \phi_{0x^*}) \phi_{0y^*} \phi_{0x^*y^*} + \left(\frac{a^2}{U_\infty^2} - \phi_{0y^*}^2 \right) \phi_{0y^*y^*} = 0 \tag{64}$$

and the Bernoulli equation

$$h(\rho, s_\infty) + \tfrac{1}{2} U_\infty^2 \left((1 + \phi_{0x^*})^2 + \phi_{0y^*}^2 \right) = h_\infty + \tfrac{1}{2} U_\infty^2. \tag{65}$$

Here the speed of sound $a(x^*, y^*)$ is calculated from the thermodynamic relation between a and h. The boundary condition (5) over the airfoil surface becomes, in the leading order,

$$\phi_{0y^*} \left(x^*, y^* = \pm 2g\, x^{*1/2} \right) \mp \frac{g}{x^{*1/2}} \left[1 + \phi_{0x^*} \left(x^*, y^* = \pm 2g\, x^{*1/2} \right) \right] = 0. \tag{66}$$

The far-field condition for the inner problem is $(\phi_{0x^*}, \phi_{0y^*}) \to 0$ as $x^* \to -\infty$. The problem given by (64)–(66) describes, in the (x^*, y^*)-plane, a sonic uniform flow $U_\infty \boldsymbol{e}_{x^*}$ around an infinite parabola surface $y^* = \pm 2g\, x^{*1/2}$ (see figure 5). The far-field behaviour of the ϕ_0 as $|x^*| \to \infty$ or $|y^*| \to \infty$ has to be specified in order to obtain a well-defined inner problem.

In the far field of the inner region, and only there, we expect that the inner flow disturbances are relatively small compared to the uniform-stream properties. Specifically, we expect that $\phi_{0x^*} \ll 1$ and $\phi_{0y^*} \ll 1$. Therefore, we can approximate

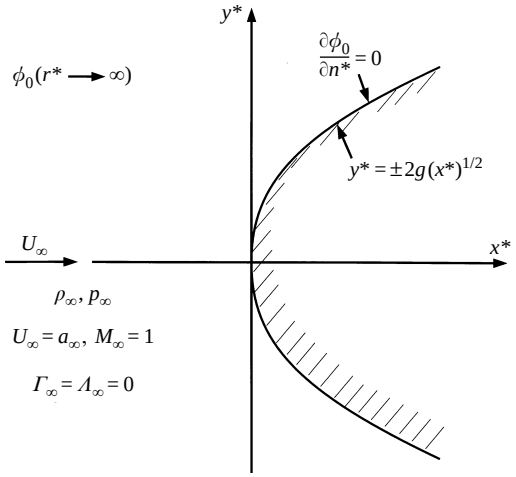

FIGURE 5. Parabolic-nose problem (the inner problem).

the speed of sound in the far field of the inner region by

$$\frac{a^2}{U_\infty^2} = \left(1 + 2\phi_{0x^*} + \phi_{0x^*}^2 - \tfrac{1}{3}\Sigma_\infty \phi_{0x^*}^3\right) + O(\epsilon^{2/5}). \tag{67}$$

Therefore, as $|x^*| \to \infty$ or $|y^*| \to \infty$, equation (64) becomes

$$\begin{aligned}\phi_{0y^*y^*} - E\ \phi_{0x^*}^3 \phi_{0x^*x^*} = {} & 2\phi_{0y^*}\phi_{0x^*y^*} + 2\phi_{0x^*}\phi_{0y^*}\phi_{0x^*y^*} \\ & -2\phi_{0x^*}\phi_{0y^*y^*} - \phi_{0x^*}^2\phi_{0y^*y^*} + E\ \phi_{0x^*}^3\phi_{0y^*y^*} + \phi_{0y^*}^2\phi_{0y^*y^*}.\end{aligned} \tag{68}$$

As $|x^*|$, $|y^*|$ increase, the potential function, ϕ_0, is assumed to be a weakly nonlinear function given by a basic function ϕ_{00} and a correction function ϕ_{01}, where $\phi_{00} \gg \phi_{01}$,

$$\phi_0(x^*, y^*) \sim \phi_{00}(x^*, y^*) + \phi_{01}(x^*, y^*). \tag{69}$$

The function ϕ_{00} is found from

$$\left.\begin{aligned} E\ \phi_{00x^*}^3\phi_{00x^*x^*} - \phi_{00y^*y^*} &= 0, \\ \phi_{00y^*}\left(x^*, y^* = \pm 2g\, x^{*1/2}\right) &= \pm\frac{g}{x^{*1/2}}, \\ (\phi_{00x^*}, \phi_{00y^*}) \to 0 \ \text{ as } \ (|x^*|,\ |y^*| &\to \infty). \end{aligned}\right\} \tag{70}$$

It can be shown that the solution of (70) is

$$\phi_{00} = E^{-1/3} y^{*8/13} f(\xi^*) \ \text{ where } \ \xi^* = \frac{x^*}{y^{*10/13}}. \tag{71}$$

Here f and $\xi^*(=\xi)$ are given by (60) (see the outer expansion). It can also be shown that the function ϕ_{01} changes like $y^{*6/13}$ as $|y^*|$ increases, which proves the assumption in (69). This result actually shows that in the far field of the inner region the flow is sonic, $K = 0$, and also characterized by the thermodynamic conditions $K_\Gamma = K_\Lambda = 0$.

From (63), (69) and (71), the potential Φ in the inner region can be approximated, as $(\epsilon \to 0, M_\infty \to 1, \Gamma_\infty \to 0, \Lambda_\infty \to 0)$ with $(x^*, y^*; K, K_\Gamma, K_\Lambda, \Sigma_\infty, \Theta)$ fixed, and as $(|x^*|, |y^*|) \to \infty$, by the asymptotic expansion

$$\Phi(x, y) = U_\infty c\epsilon^2 \left(x^* + E^{-1/3} y^{*8/13} f(\xi^*) + \ldots\right) + \ldots. \tag{72}$$

To summarize the inner problem, the potential Φ in the inner region is governed by equations (64) and (65), boundary condition (66) and far-field behaviour (72). This problem, in the inner region, describes an oncoming uniform sonic flow with the thermodynamic properties $\Gamma_\infty = \Lambda_\infty = 0$ around an infinite parabola surface.

5. Matching

The matching of the outer and inner asymptotic expansions is carried out with the help of an intermediate region. There, $x_\eta = \bar{x}/\eta(\epsilon)$, $y_\eta = \bar{y}/\eta(\epsilon)$ are fixed in the limit ($\epsilon \to 0, M_\infty \to 1, \Gamma_\infty \to 0, \Lambda_\infty \to 0$) as well as the parameters $(K, K_\Gamma, K_\Lambda, \Sigma_\infty, \Theta)$. The region $\eta(\epsilon)$ is chosen such that $\epsilon^2 \ll \eta(\epsilon) \ll 1$, and as $\epsilon \to 0$, $\eta(\epsilon)/\epsilon^2 \to \infty$. Then $\bar{x} = \eta(\epsilon)x_\eta \to 0$ and $\tilde{y} = \eta(\epsilon)\epsilon^{3/5}y_\eta \to 0$ whereas $|x^*| = (\eta(\epsilon)/\epsilon^2)\,|x_\eta| \to \infty$ and $|y^*| = (\eta(\epsilon)/\epsilon^2)\,|y_\eta| \to \infty$. Also, we can show that $\xi = \xi^*$. The region $\eta(\epsilon)$ represents a whole-order class of limits between the inner and outer and is called the overlap region. For matching, the expansions must read the same to a certain order when expressed in the (x_η, y_η) coordinates. From (62) and (72) we find that:

outer expansion

$$\Phi(x, y) = U_\infty c \left\{ \eta x_\eta + \epsilon^{2/5} E^{-1/3} \left(\epsilon^{3/5} \eta y_\eta\right)^{8/13} f(\xi) + \ldots \right\}$$

$$\Leftrightarrow$$

inner expansion

$$\Phi(x, y) = U_\infty c \epsilon^2 \left\{ \frac{\eta x_\eta}{\epsilon^2} + E^{-1/3} \left(\frac{\eta y_\eta}{\epsilon^2}\right)^{8/13} f(\xi^*) + \ldots \right\}.$$

It is clear that the leading terms in the two expansions match. The matching between the expansions shows a uniform behaviour of the potential Φ as well as the thermodynamic flow properties between the inner and outer regions.

6. Numerical solution of the inner problem

The inner potential flow problem described by (64)–(66) and (72) is equivalent to solving the Euler equations of an oncoming uniform sonic flow with $\Gamma_\infty = \Lambda_\infty = 0$ around an infinite parabola surface. We used the two-dimensional and steady Euler equations numerical solver from Morren (1990). This computer code is a modified version of Jameson & Yoon's (1986) FLO52 finite volume code to enable modelling the flow of a dense retrograde gas near the saturated vapour curve and the critical pressure region. In this code the thermodynamic equation of state is described by the van der Waals equation (see, for example, Moran & Shapiro 1992)

$$p = \frac{\rho R T}{1 - b\rho} - \alpha \rho^2. \tag{73}$$

Here R is the gas constant, $R = \bar{R}/M$ ($\bar{R}$ is the universal gas constant and M is the gas molecular weight). The coefficients α and b are corrections for the intermolecular forces of attraction and repulsion between the molecules, and for the volume occupied by the molecules. These coefficients can be evaluated from the thermodynamic critical point data (p_c, ρ_c) of the substance,

$$\alpha = \frac{27}{64} \frac{R^2 T_c^2}{p_c}, \quad b = \frac{1}{8} \frac{R T_c}{p_c} = \frac{1}{3\rho_c}.$$

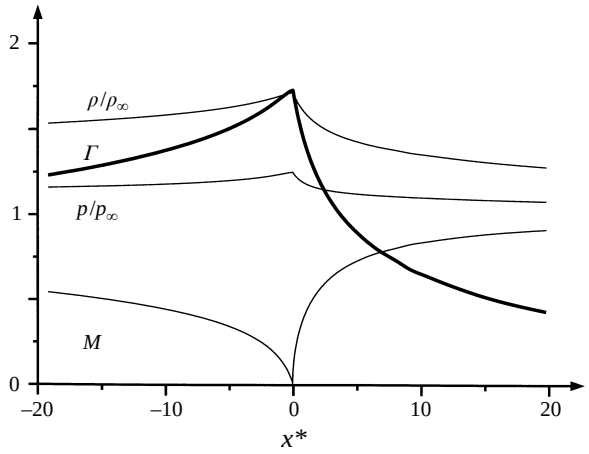

FIGURE 6. Numerical solution of sonic flow around the parabola surface.

The critical compressibility factor, Z_c, for van der Waals gases is

$$Z_c = \frac{p_c}{RT_c\rho_c} = 0.375.$$

The analysis of Morren (1990) also assumes that the specific heat for constant volume, c_v, is constant for all pressures and densities.

For the case of the inner flow problem where $\Gamma_\infty = \Lambda_\infty = 0$, we can show (see the Appendix) that

$$\bar{\alpha} = \frac{\alpha\rho_\infty^2}{p_\infty} = \frac{16\left(1 + R/c_v\right)\left(1 + R/2c_v\right)}{11\left(1 - R/c_v\right)\left(1 + 5R/11c_v\right)}, \quad \bar{b} = b\rho_\infty = \frac{1 - R/c_v}{4} \tag{74}$$

and using the critical compressibility factor we then have the oncoming uniform flow with density and pressure in the form

$$\frac{\rho_\infty}{\rho_c} = 3\bar{b}, \quad \frac{p_\infty}{p_c} = 27\frac{\bar{b}^2}{\bar{\alpha}}. \tag{75}$$

The numerical solution of the oncoming sonic flow with $R/c_v = 0.02$ (or with $\rho_\infty/\rho_c = 0.735$, $p_\infty/p_c = 1.0696$) around the parabola surface results in the pressure, density, Mach number and Γ distributions shown in figure 6. In this figure the results are presented along the x^*-axis when $x^* < 0$ and over the parabola surface when $x^* > 0$. We can see that the flow is subsonic everywhere. It decelerates to stagnation at the parabola nose and then accelerates back to sonic flow. The pressure, density and Γ increase to their stagnation values at the parabola leading edge and then decrease back to their far-field values.

Figure 7 shows the comparative calculations of the pressure ratio, Mach number and Γ between the parabolic configuration and the NACA0012 airfoil given for a uniform stream with $M_\infty = 1.0$, $\Gamma_\infty = \Lambda_\infty = 0$, $R/c_v = 0.02$ and zero angle of attack. In this figure the solution of the various parameters are given along the $(-x)$-axis when $x < 0$ and over the surfaces when $x > 0$. It is recognized that these two sets of solutions have similar distributions of each property up to about $x/c = 0.1$. In a region around the leading edge of about 2% of the airfoil's chord, which is of the order of the size of the inner region, the parabola solution is especially close to the solution of the Euler equations. These results suggest that, indeed, in the inner region

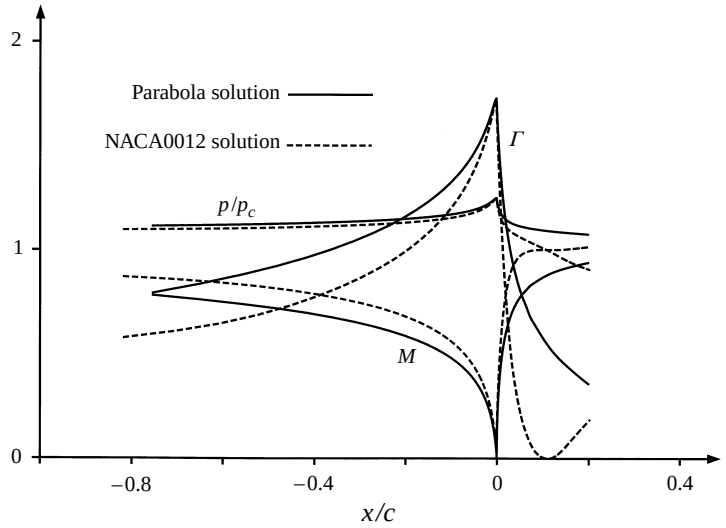

FIGURE 7. Comparison of the solutions of a sonic flow around a parabola and around a NACA0012 airfoil in the nose region.

the solution of the Euler equations for the airfoil is dominated by the solution of the parabola problem.

7. A uniformly valid solution

A uniformly valid solution for the potential Φ can be constructed from the outer and inner expansions, by adding the two together and subtracting the common part in the intermediate region where the two solutions match. The composite solution is given by

$$\Phi(x,y;\epsilon,M_\infty,\Theta,\Gamma_\infty,\Lambda_\infty,\Sigma_\infty) \sim U_\infty c\left\{\bar{x}+\epsilon^{2/5}\bar{\phi}_1(\bar{x},\tilde{y};K,K_\Gamma,K_\Lambda,\Sigma_\infty) + \epsilon^2\left(x^*+\phi_0(x^*,y^*)\right)-\Phi_{c.p.}\right\} \tag{76}$$

where the common part is

$$\Phi_{c.p.} = \eta x_\eta + E^{-1/3}\eta^{8/13}\epsilon^{10/13}y_\eta^{8/13} f\left(\left(\frac{\eta}{\epsilon^2}\right)^{3/13}\xi_\eta\right), \quad \xi_\eta = \frac{x_\eta}{y_\eta^{10/13}}. \tag{77}$$

From the composite solution (76) and (77) and the Bernoulli equation (8) the enthalpy in the flow field may be approximated by

$$\frac{h-h_\infty}{a_\infty^2} = \frac{h^*(x^*,y^*)-h_\infty}{a_\infty^2} + \left(1+\phi_{0x^*}(x^*,y^*)\right)\frac{h_{TSD}-h_{c.p.}}{a_\infty^2}+\ldots \tag{78}$$

where $h^*(x^*,y^*)$ and $(1+\phi_{0x^*}(x^*,y^*))$ are the enthalpy and axial velocity component in the inner flow problem, respectively. Also, $(h_{TSD}-h_\infty)/a_\infty^2 = -\epsilon^{2/5}\bar{\phi}_{1\bar{x}}$ is the enthalpy in the outer (transonic small-disturbance) flow problem and $(h_{c.p.}-h_\infty)/a_\infty^2 = -\epsilon^{2/5}E^{-1/3}\tilde{y}^{-2/13}f_\xi$ is the enthalpy of the common part in the overlap region. Equation (78) shows that the enthalpy at any point is composed of two main effects of the parabola problem and the small-disturbance problem. As the leading edge of the airfoil is approached, $(x,y)\to 0$ or $(x^2+y^2)^{1/2} < \epsilon^2 g^2 c$, the common-part enthalpy ($h_{c.p.}$) cancels the nose singularity of the outer-region enthalpy. Also, in this region

the axial velocity $(1 + \phi_{0x^*}(x^*, y^*))$ is small and tends to zero near the stagnation point. Therefore, the dominant term in the leading-edge region is the inner-region enthalpy h^*. As (x, y) increase beyond the leading-edge region ($(x^2 + y^2)^{1/2} \gg \epsilon^2 g^2 c$), the axial velocity $(1 + \phi_{0x^*}(x^*, y^*))$ tends to 1 and the common-part enthalpy cancels the inner-region enthalpy (h^*). Therefore, the dominant term outside the leading-edge region is the transonic small-disturbance term (h_{TSD}). In the intermediate region the enthalpy changes uniformly from h^* to h_{TSD}.

From the solution of the enthalpy (78) and the thermodynamic relations $h(\rho, s_\infty)$ and $p(\rho, s_\infty)$, we can approximate first the distribution of density and then pressure in the entire flow field. These thermodynamic relations, however, may be relatively complicated and, therefore, no general formula is given to approximate the density and pressure. For the case where the van der Waals equation of state is used these relations are given in the Appendix.

8. Conclusions

The transonic flow of BZT gases around a thin airfoil with a parabolic nose can be analysed by matched asymptotic methods. Asymptotic expansions of the velocity potential function are constructed in terms of the airfoil thickness ratio at an outer region around the airfoil and in an inner region near the nose. The outer expansion consists of the transonic small-disturbance theory for BZT gases of Tarkenton & Cramer (1993). Similarity solutions of the governing nonlinear equation (which is a modified version of the Kármán–Guderley equation) are found using a transformation to the hodograph plane. Analytical expressions are given for the leading-edge singularity in the outer expansion of the pressure and the fundamental derivative of gasdynamics (see equations (60) and (61)). A well-defined inner problem that matches the outer expansion is constructed. In the inner region near the nose of the airfoil, of a radius of $\epsilon^2 g^2 c$, the flow can be approximated by the solution of an oncoming uniform sonic flow with $\Gamma_\infty = \Lambda_\infty = 0$ around an infinite parabola surface. The numerical solution of the inner flow results in symmetric pressure, density, Mach number and Γ distributions on the parabolic nose. The flow near the airfoil leading edge is subsonic without any sonic or supersonic shock waves. From the outer and inner solutions a uniformly valid solution of the flow field around the entire airfoil can be given. This composite solution is relatively simple and provides a good approximation to the solution of the Euler equations, specifically of the enthalpy and pressure distributions over the airfoil.

The authors would like to thank Professor Mark S. Cramer for providing them with the computer code of Morren (1990). The second author (C.-W. Wang) wishes to thank the Chung–Cheng Institute of Technology (CCIT) in Taiwan for supporting his graduate studies.

Appendix

We derive here the thermodynamic fundamental derivative, Γ, and the second derivative, Λ, for a van der Waals gas. The general form of entropy in terms of the pressure, temperature and density is given by

$$\mathrm{d}s = c_v \frac{\mathrm{d}T}{T} + \left(\frac{\partial p}{\partial T}\right)_\rho \frac{\mathrm{d}\rho}{\rho^2}.$$

From the van der Waals equation of state (73) we have

$$\left(\frac{\partial p}{\partial T}\right)_{\rho} = \frac{\rho R}{1-b\rho},$$

and so

$$\mathrm{d}s = c_v \frac{\mathrm{d}T}{T} - \left(\frac{R}{1-b\rho}\right)\frac{\mathrm{d}\rho}{\rho}.$$

Integrating this equation with respect to a reference state where $\rho_r = \rho_\infty$ and $s_r = s_\infty$, we have

$$\frac{s-s_\infty}{c_v} = \ln\left(\frac{T}{T_\infty}\right) + \frac{R}{c_v}\ln\left[\left(\frac{1-b\rho}{\rho}\right)\left(\frac{\rho_\infty}{1-b\rho_\infty}\right)\right].$$

Here, from (73)

$$T_\infty = \frac{(1-b\rho_\infty)(p_\infty + \alpha\rho_\infty^2)}{\rho_\infty R}.$$

Using the definitions

$$\bar{\rho} = \frac{\rho}{\rho_\infty},\ \bar{p} = \frac{p}{p_\infty},\ \bar{a}^2 = \frac{a^2}{a_\infty^2},\ \bar{\alpha} = \frac{\alpha\rho_\infty^2}{p_\infty},\ \bar{b} = b\rho_\infty,$$

the entropy equation is

$$\bar{s} \equiv \exp\left(\frac{s-s_\infty}{c_v}\right) = \left(\bar{\rho}\frac{1-\bar{b}}{1-\bar{b}\bar{\rho}}\right)^{1+R/c_v}\left(\frac{1+\bar{\alpha}}{\bar{p}+\bar{\alpha}\bar{\rho}^2}\right).$$

Thus, the non-dimensional pressure is

$$\bar{p} = \left(\frac{1+\bar{\alpha}}{\bar{s}}\right)\left(\bar{\rho}\frac{1-\bar{b}}{1-\bar{b}\bar{\rho}}\right)^{1+R/c_v} - \bar{\alpha}\bar{\rho}^2.$$

From this relation the non-dimensional speed of sound is

$$\bar{a}^2 \equiv \left(\frac{\partial\bar{p}}{\partial\bar{\rho}}\right)_{\bar{s}} = \left(\frac{\bar{p}+\bar{\alpha}\bar{\rho}^2}{\bar{\rho}(1-\bar{b}\bar{\rho})}\right)\left(1+\frac{R}{c_v}\right) - 2\bar{\alpha}\bar{\rho} = (1-\bar{b}\bar{\rho})^{-2-R/c_v}\bar{\rho}^{R/c_v}N - 2\bar{\alpha}\bar{\rho}$$

where

$$N = \left(\frac{1+\bar{\alpha}}{\bar{s}}\right)(1-\bar{b})^{1+R/c_v}\left(1+\frac{R}{c_v}\right) = \text{constant}.$$

Therefore,

$$\left.\frac{\partial\bar{a}}{\partial\bar{\rho}}\right|_{\bar{s}} = \frac{N}{2\bar{a}}\bar{\rho}^{R/c_v}(1-\bar{b}\bar{\rho})^{-3-R/c_v}\left(2\bar{b}+\frac{R}{c_v\bar{\rho}}\right) - \frac{\bar{\alpha}}{\bar{a}}$$

and the fundamental derivative of gasdynamics, Γ, is

$$\Gamma = \frac{\bar{\rho}}{\bar{a}}\left\{N\bar{\rho}^{R/c_v-2}(1-\bar{b}\bar{\rho})^{-3-R/c_v}\left(1+\frac{R}{2c_v}\right) - 3\frac{\bar{\alpha}}{\bar{\rho}}\right\}.$$

At the far field, where $\bar{\rho} = \bar{p} = \bar{s} = 1$ and $\Gamma_\infty = 0$, we have

$$\bar{b} = 1 - \left[\left(\frac{1+\bar{\alpha}}{3\bar{\alpha}}\right)\left(1+\frac{R}{c_v}\right)\left(1+\frac{R}{2c_v}\right)\right]^{1/2}.$$

Also, from the formula for Γ,

$$\Lambda = \frac{\partial \Gamma}{\partial \bar{\rho}} = -\frac{\Gamma}{\bar{a}} + \frac{N}{\bar{a}}\bar{\rho}^{R/c_v-2}(1-\bar{b}\bar{\rho})^{-4-R/c_v}\left(1+\frac{R}{2c_v}\right)\left(\frac{R}{c_v}-1+4\bar{b}\bar{\rho}\right).$$

For the far-field conditions of $\Gamma_\infty = \Lambda_\infty = 0$, we find

$$\bar{b} = \frac{1-R/c_v}{4}$$

and

$$\bar{\alpha} = \frac{16\left(1+R/c_v\right)\left(1+R/2c_v\right)}{11\left(1-R/c_v\right)\left(1+5R/11c_v\right)}.$$

Also, the general form of the internal energy (u) in terms of the pressure, temperature and density is given by

$$\mathrm{d}u = c_v \mathrm{d}T - \left(T\frac{\partial p}{\partial T}_{\rho} - p\right)\frac{\mathrm{d}\rho}{\rho^2}.$$

For the van der Waals gas model with the assumption of a constant c_v, we find

$$u - u_\infty = c_v(T - T_\infty) - \alpha(\rho - \rho_\infty)$$

and from enthalpy definition

$$h - h_\infty = c_v T_\infty\left(\frac{T}{T_\infty}-1\right) - 2\alpha(\rho-\rho_\infty) + \frac{RT_\infty}{1-b\rho_\infty}\left(\frac{T}{T_\infty}\frac{1-b\rho_\infty}{1-b\rho}-1\right).$$

Using the van der Waals equation (73) and the formula for $\bar{p}$ derived above, we can compute

$$\left.\frac{T}{T_\infty}\right|_{s=s_\infty} = \left(\frac{\rho}{\rho_\infty}\frac{1-b\rho_\infty}{1-b\rho}\right)^{R/c_v}$$

from which the enthalpy as function of density in an isentropic flow $s = s_\infty$ can be computed.

REFERENCES

Abbott, I. H. & Doenhoff, A. E. von 1959 *Theory of Wing Sections*. Dover.

Abramowitz, M. & Stegun, I. A. 1965 *Handbook of Mathematical Functions*. Dover.

Bethe, H. A. 1942 The theory of shock waves for an arbitrary equation of state. *Office of Scientific Research and Development, Rep.* 545.

Cramer, M. S. 1989 Negative nonlinearity in selected fluorocarbons. *Phys. Fluids* A **1**, 1894–1897.

Cramer, M. S. 1991 On the Mach number variation in steady flows of dense hydrocarbons. *Trans. ASME: J. Fluids Engng* **113**, 675–680.

Cramer, M. S. & Best, L. M. 1991 Steady, isentropic flows of dense gases. *Phys. Fluids* A **3**, 219–226.

Cramer, M. S. & Fry, R. 1993 Nozzle flows of dense gases. *Phys. Fluids* A **5**, 1246–1259.

Cramer, M. S. & Tarkenton, G. M. 1992 Transonic flows of Bethe-Zel'dovich-Thompson fluids. *J. Fluid Mech.* **240**, 197–228.

Devotta, S. & Holland, F. A. 1985 Comparison of theoretical Rankine power cycle performance data for 24 working fluids. *Heat Recovery Syst.* **5**, 503.

Duhem, P. 1909 Sur la propagation der ondes de choc au sien des fluids. *Z. Phys. Chem., Leipzig* **69**, 169–186.

Jameson, A. & Yoon, S. 1986 Multigrid solution of the Euler equations using implicit schemes. *AIAA J.* **24**, 1737–1743.

KLUWICK, A. 1993 Transonic nozzle flow in dense gases. *J. Fluid Mech.* **247**, 661–688.

MARTIN, J. J. & HOU, Y. C. 1955 Development of an equation of state for gases. *AIChE J.* **1**, 142–151.

MORAN, M. J. & SHAPIRO, H. N. 1992 *Fundamentals of Engineering Thermodynamics*, 3rd Edn. John Wiley & Sons.

MORREN, S. H. 1990 Transonic aerodynamics of dense gases. MSc thesis, Engineering Science and Mechanics Department, Virginia Polytechnic Institute and State University (also *NASA TM* 103732, 1991).

REDLICH, O. & KWONG, J. N. S. 1949 On the thermodynamics of solutions V. An equation of state fugacities of gaseous solutions. *Chem. Rev.* **44**, 233.

RUSAK, Z. 1993 Transonic flow around the leading edge of a thin airfoil with a parabolic nose. *J. Fluid Mech.* **248**, 1–26.

SCHNERR, G. H. & LEIDNER, P. 1993 Real gas effects on the normal shock behavior near curved walls. *Phys. Fluids* **5**, 2996–3003.

TARKENTON, G. M. & CRAMER, M. S. 1993 Transonic flows of regular dense gases. *ASME Paper* 93-FE-9.

THOMPSON, P. A. 1971 A fundamental derivative in gasdynamics. *Phys. Fluids* **14**, 1843–1849.

THOMPSON, P. A. 1984 *Compressible Fluid Dynamics.* Advanced Engineering Series.

THOMPSON, P. A. & LAMBRAKIS, K. 1973 Negative shock waves. *J. Fluid Mech.* **60**, 187–208.

ZEL'DOVICH Y. B. 1946 On the possibility of rarefaction shock waves. *Zh. Eksp. Teor. Fiz.* **4**, 363–364.

ZEL'DOVICH Y. B. & Raizer, Y. P. 1966 *Physics of Shock Waves and High Temperature Hydrodynamic Phenomena.* Academic.